^{1}H NMR Study of Dispersion Copolymerization of *n*-Butyl Methacrylate with Poly(ethylene oxide) Macromonomer in Deuterated Methanol−Water

Seigou Kawaguchi[1] and Mitchell A. Winnik*

Department of Chemistry and Erindale College, University of Toronto, Toronto, Ontario, Canada M5S 1A1

Koichi Ito

Department of Materials Science, Toyohashi University of Technology, Tempaku-cho, Toyohashi 441 Japan

Received May 26, 1995; Revised Manuscript Received March 29, 1996[⊗]

ABSTRACT: ^{1}H NMR and dynamic light scattering (DLS) measurements have been employed to investigate the dispersion copolymerization of *n*-butyl methacrylate (BMA) with poly(ethylene oxide) (PEO) macromonomer in a deuterated methanol−water medium. During the first quarter of the polymerization BMA and the macromonomer react at nearly the same polymerization rate. Subsequently, the BMA polymerization rate increases markedly, due to partitioning of the BMA into the particle phase. When this occurs, one observes broadening of the ^{1}H NMR absorption lines of the unreacted BMA. The PEO peak intensity was monitored relative to that of an internal standard. As conversion proceeds, the sharp peak represents a superposition of signal due to unreacted macromonomer and to chains attached to the particle which maintain their high mobility. ^{1}H signals from immobilized EO segments appear as a weak broad background which grows in intensity as the reaction proceeds. At the end of the reaction, 27% of the intensity in the sharp PEO resonance is lost, implying that this fraction of the chain segments have become immobilized due to surface adsorption or entrapment within the particle interior. From these data, the amount of PEO bound to the surface as a function of the extent of reaction can be calculated. This in turn suggests that there is a sharp increase, toward the end of the reaction, in the fraction of EO chain segments which have high mobility and appear in the NMR with a narrow line shape. Calculated packing densities are consistent with a transition to a brushlike conformation of the PEO chains.

Introduction

Dispersion polymerization is a type of precipitation polymerization in which one carries out the polymerization of a monomer in the presence of a second polymer soluble in the reaction medium.[2,3] The polymerization affords polymer particles 0.1−15 μm in diameter, often of excellent monodispersity. This second polymer can be a macromonomer, as in the case described here. It can be a block copolymer in which one block has an affinity for the surface of the precipitated polymer, or it can be a soluble polymer (a "stabilizer precursor") to which grafting occurs during the polymerization reaction. In all instances, this soluble polymer plays a crucial role in the dispersion polymerization process. By adsorbing or becoming incorporated into the surface of the newly formed precipitated polymer, it acts as a steric stabilizer to provide colloidal stability to the system. This feature of dispersion polymerization is widely appreciated and relatively well understood.

While it is clear that some or most of the soluble polymer must be on the particle surface to provide steric stabilization, it is also possible that some of this polymer becomes buried in the particle interior during the polymerization reaction. The amount that is buried is normally very difficult to determine. One appraoch is to label the stabilizer or stabilizer precursor with a fluorescent dye and then to prepare particles containing the label in the stabilizer component.[4,5] If a quencher is added to the system, and if the quencher is confined to the continuous medium, it will quench only those chromophores accessible to the solvent. Buried chromophores will be protected against quenching. From the amount of unquenchable chromophore, one can infer the fraction of buried stabilizer.

Here we take a different approach. We have been interested in dispersion polymerization in the presence of poly(ethylene oxide) [PEO] macromonomer (**1**) to prepare latex particles with PEO chains at their surface.

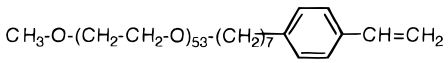

(**1**) C_1-EO_{53}-C_7-S

In a previous paper,[6] we examined its dispersion copolymerization with *n*-butyl methacrylate [BMA] in methanol−water mixtures. Factors which affect the particle size include the structure and molecular weight of macromonomers, the initial concentrations of BMA, initiator, and macromonomer, temperature, and the composition of the solvent.

The true steric stabilizer in the system is poly(BMA-*graft*-PEO) synthesized in situ during the dispersion copolymerization. To describe the mechanism of the polymerization reaction, and to interpret the kinetics in terms of Paine's multibin kinetics model,[7] we needed to know what fraction, if any, of the PEO stabilizer chains was buried in the particle. It occurred to us that we could follow the incorporation and the locus of these chains in the system by ^{1}H NMR if we carried out the reaction in deuterated solvent. Small molecules and polymers in solution which undergo rapid motion give sharp peaks in the NMR, whereas polymers in the solid state have very broad lines which often disappear into the baseline.[8]

* To whom correspondence should be addressed.
[⊗] Abstract published in *Advance ACS Abstracts,* May 15, 1996.

S0024-9297(95)00726-1 CCC: $12.00

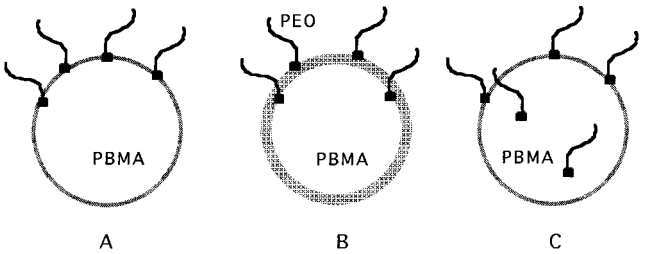

Figure 1. Representations of possible structures for the PBMA particles sterically stabilized by PEO chains grafted at the surface. In A, all chains have the copolymerized styrene unit at the surface of the particle, so that all EO segments might have high mobility. In B, the particle surface structure is diffuse because of solvent swelling, promoted perhaps by the presence of the PEO graft copolymer. Some macromonomer chains are attached deep within this layer so that EO units in this environment might have restricted mobility. In C, some of the macromonomer chains form graft copolymer molecules which are buried inside the particle. Other PEO grafts remain at the surface.

In Figure 1 we present drawings of three possible structures for the PBMA particles. In A, the particle is shown as a hard sphere with a well-defined surface, and with the chain ends of the macromonomer attached at the surface. Here, with the possible exception of a few EO units next to the styrene end of the molecule, the polymer segments should all be rather mobile. In C, we imagine a similar particle surface but consider that the particle formation mechanism may somehow result in some PEO grafts being buried inside the particle. Here the buried fraction of PEO chains are confined to a domain of restricted mobility. In B, we envision a third possible immobilization mechanism. The presence of the PEO graft copolymer may make the surface layer of the particle more swellable by solvent. If this were to occur, the particle would have a diffuse interface at the surface, with a gradient of mobility for groups between the polymer edge and the solvent edge of this domain.

Our idea for the NMR experiment is based upon concepts that have been studied extensively for more than 20 years and have been reviewed recently by Blum,[9] and in more detail by Cosgrove and Griffiths,[8] and by Fleer et al.[10] When polymers in solution adsorb onto a surface, there is a decrease in intensity in the high-resolution NMR peaks associated with the mobile segments of the polymer. Processes leading to T_2 relaxations average the dipolar coupling. Where separate populations of bound and unbound polymer segments occur, the immobilized segments appear as broad peaks or broad background in the spectra. In high-resolution ^{1}H NMR, peak broadening can be so extensive compared to the width of the peaks in the system due to mobile species, that the signal from the immobilized segments cannot be distinguished from the background.

Many experiments have been reported involving the interaction of PEO with silica particle surfaces. These experiments involved polymer adsorption from solution, as well as particles with end-grafted chains. Two types of information were sought: the amount of polymer bound to the particles and the nature of the binding. Here one tries to assess the extent to which the bound chains are present as trains attached to the surface, and the fraction of segments contained within loops and tails protruding into the solvent.

A wide variety of experiments, including neutron and dynamic light scattering measurements, indicate that when the amount of polymer added to the system is small, the chains lie largely flat on the surface. Here, as much as 90% of the signal in the ^{1}H NMR can be "lost" from the spectrum.[11] With additional added polymer, the packing density on the surface increases, as does the fraction of polymer segments which appear as a sharp peak in the spectrum. At these densities, a larger fraction of the polymer is present as loops and tails. At high packing densities, there is a sharp transition to a conformation in which the tails extend far into the continuous medium. In the polymer physics literature, this process is referred to as a pancake-to-brush transition:[12] at low concentrations, the chains lie flat like a pancake on the surface, whereas at higher packing, repulsions between the solvent-swollen polymer chains lead to chain stretching in the direction perpendicular to the surface.

In some systems, high-resolution NMR measurements give a higher fraction of immobilized chain segments than that obtained from infrared (IR) spectroscopy measurements. IR measures the direct interaction of functional groups in the segments with the surface, through, for example, hydrogen bonding. The NMR results are less local and are sensitive to the reduced mobility of segments near the surface that are not directly interacting with it. Thus, if the polymer chains are relatively stiff, one finds a higher "bound fraction" by NMR than by IR.[10]

Our system is somewhat more complicated than the polymer-plus-silica systems in two respects. First, in our system, there are proton signals from other components. Second, we have to consider both passive adsorption of PEO onto the particle surfaces and covalent incorporation of the PEO chain ends into the particles through the copolymerization process. To quantify the fate of the PEO polymer, we focus on the sharp peak in the ^{1}H NMR at 3.64 ppm due to the highly mobile EO segments. A challenge to us in interpreting the data is to see to what extent we can separate adsorption onto the latex particle surface from burial inside the particle as a source of PEO immobilization.

In ^{1}H NMR spectra taken before the reaction (cf., Figure 2), the BMA and the PEO macromonomer both exhibit sharp peaks. We expected that the vinylic protons of the BMA and macromonomer would disappear as the polymerization proceeds, providing a means to study the kinetics of the polymerization. On the other hand, we anticipated that peaks due to the protons of PBMA would not be prominent in the spectrum, due to immobilization as PBMA forms a separate particle phase. The data bear this out. One interesting observation is a broadening of the signals due to the BMA monomer at about 50% conversion, suggesting a partitioning of the BMA from the continuous phase into the particles.

We are primarily interested the effect of polymerization of the macromonomer on the PEO proton signal. As described above, we anticipated a decrease in the intensity of the sharp peak due to the mobile PEO component as portions of the polymer become immobilized by surface adsorption or entrapment within the particle. In the sections that follow, we describe the experiments and examine their implications on the dispersion polymerization mechansim. We also discuss the conformational properties of terminally-attached PEO chains.

We find at the end of the reaction two distinct PEO proton signals, the sharp peak at 3.64 ppm sitting atop a very broad signal likely due to segments of restricted

Table 1. Recipe for the Dispersion Copolymerization[a]

C_1-EO_{53}-C_7-S	0.1003 g	0.040 mmol
BMA	1.2006 g	8.44 mmol
AIBN	0.0250 g	0.15 mmol
PCA	0.0676 g	0.40 mmol
methanol-d_4	8.0 mL	
H_2O-d_2	2.0 mL	

[a] A 1.5 mL aliquot of this solution was used for one batch of the dispersion copolymerization.

mobility. By comparing the intensity within the sharp peak to the extent of macromonomer conversion, we can estimate what fraction of the bound PEO segments have become immobilized. This fraction is remarkably high at early stages of the reaction (ca. 80% at 20% conversion), and much smaller at later conversions. From independent information on particle number and particle size, and some assumptions about the behavior of the unreacted macromonomer, we can estimate the mean spacing of end-grafted chains on the particle surface. When this density is low, during early stages of the reaction, it appears that the PEO chains tend to lie flat on the surface. As this chain spacing decreases, we find a sharp increase in the fraction of segments of end-grafted PEO which are mobile. This can be interpreted as a transition to a brushlike structure for the chains attached to the particle surface.

Experimental Section

Materials. The PEO macromonomer (**1**) (C_1-EO_{53}-C_7-S) was prepared and characterized by the method reported in previous papers.[6] BMA (Aldrich) was distilled just before use. D-deuterated (99.96%) water (Aldrich) and 99.8% D-deuterated methanol (Aldrich) were used without further purification. α,α′-Azobis(isobutyronitrile) (AIBN, Polysciences Ltd.) was purified by recrystallization three times from ethanol. 2,3-Pyridinedicarboxylic acid (PCA, Aldrich) was used as an internal standard for the ^{1}H NMR measurements.

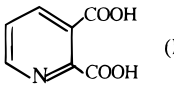

(PCA)

Dispersion Copolymerization. Dispersion copolymerizations were carried out with magnetic stirring in 5 mL one-neck reactors, each fitted with a condenser under an argon atmosphere at 70 °C. The mixture used for the dispersion copolymerization is presented in Table 1. Individual 1.5 mL aliquots were placed in a 5 mL flask, polymerized for an appropriate time, and then cooled to room temperature so that the reaction ceases. ^{1}H NMR spectra and particle size distributions were then measured for each sample.

Measurements. ^{1}H NMR spectra were run at room temperature on a Varian GEMINI 200-MHz FT NMR spectrometer. Recording conditions were 64 scans and 10−18 μs pulse widths. The chemical shifts in aqueous solution and dispersion were determined by assigning 4.78 ppm to water protons. In $CDCl_3$ tetramethylsilane was used as a reference. Peaks or regions of a spectrum were integrated using software provided with the instrument, in which the operator specifies the chemical shift intervals over which the integrations are taken. The particle diameters were measured with a dynamic light scattering photometer (DLS) (Brookhaven Instruments BI-90 Particle Sizer with 10 mW He−Ne laser) with a fixed scattering angle of 90° at 20 °C. The solvent used for DLS was spectroscopic grade methanol (Caledon Laboratories Ltd.) (viscosity = 0.597 cP) without further optical purification. Data analysis was carried out using the built in algorithm for inverse Laplace transformation. The intensity median diameter of the BI-90 measurement was used as the average diameter for the particles. As a measure of the size distribution, we used the geometric standard deviation. The values range from 1.1 to 1.2, which implies that the latex size distribution is nearly monodisperse.[6]

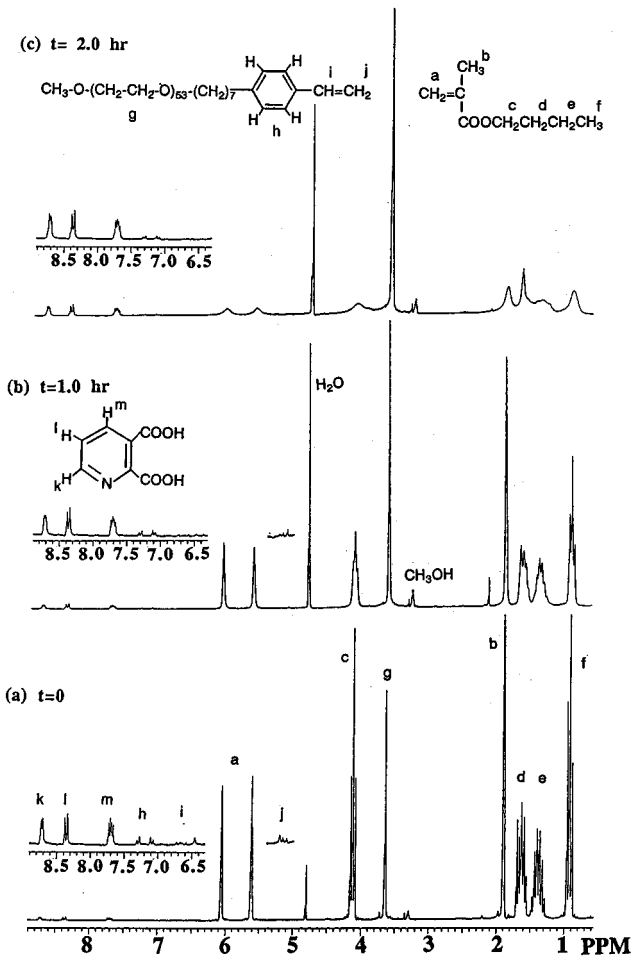

Figure 2. ^{1}H NMR spectra of BMA and C_1-EO_{53}-C_7-S before and during dispersion copolymerization: (a) $t = 0$; (b) $t = 1.0$ h; (c) $t = 2.0$ h. The assignments for each NMR peak are shown in this figure.

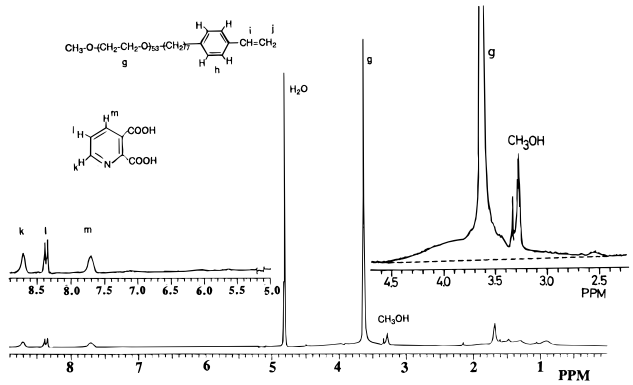

Figure 3. ^{1}H NMR spectrum of the dispersion after $t = 4$ h of polymerization.

Results and Discussion

This section is organized as follows: We first examine general features of the ^{1}H NMR spectra of the system, presenting spectra of the reaction mixture as a function of reaction time in Figures 2 and 3 and of the reaction products in a good solvent for all of the components in Figure 4. The most obvious changes that occur in the spectra involve the conversion of monomer to polymer, accompanied, for example, by the disappearance of the

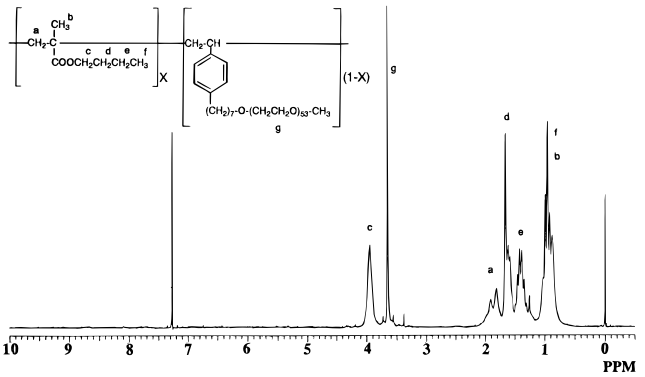

Figure 4. ^{1}H NMR spectrum of polymers after 4 h of polymerization, after dissolution of the sample in $CDCl_3$.

olefinic peaks in the region of 5−6 ppm and by changes in the CH_2O− ester group resonances (peak c) at 4.1 ppm. While these changes are important, we will focus more attention on peak g at 3.64 ppm, due to EO segments of the PEO polymer chain. Changes in the intensity of this peak, which are difficult to see in the spectra in Figure 2, become apparent in Figure 3. We try to quantify these changes and to interpret the results in terms of partial immobilization of a fraction of the PEO polymer in the system.

General Features of ^{1}H NMR Spectra. ^{1}H NMR spectra of the dispersion polymerization at various polymerization times (t) are shown in Figures 2 and 3. In all samples, a known amount of 2,3-pyridinedicarboxylic acid [PCA] serves as an internal standard. We confirmed that the ratio of the peak area of PCA protons, which appear at 7.5−9.0 ppm, to that of solvent protons (at 3.3 and 4.8 ppm) remains constant throughout the polymerization reaction. This indicates not only that PCA is stable to the reaction conditions but also that the PCA molecules exist only in the continuous phase and do not become incorporated into the particles. There are four noteworthy features of the system seen in these spectra: (1) the reaction of the double bonds of BMA and the macromonomer, (2) the disappearance of NMR peaks ascribed to the PBMA polymer, (3) the broadening of the NMR line width of the BMA resonances, and (4) the decrease in intensity of the signal due to the PEO chains which appears as a sharp peak at 3.64 ppm. We discuss each of these in turn below.

It is clear from Figures 2 and 3 that NMR peak intensities ascribed to the double bonds of BMA and the macromonomer decrease with the polymerization time, when compared to the peaks due to PCA protons. After 4 h of polymerization the ^{1}H NMR resonances ascribed to the vinylic protons of BMA and the macromonomer have completely disappeared. In Figure 3, one can observe only peaks due to PCA, solvent, PEO, and a slight amount of aliphatic hydrocarbon protons. Therefore, this methodology allows one to monitor monomer consumption during the reaction without separating polymer from unreacted monomer.

There is very little signal due to PBMA protons. This result was expected and confirms that the polymerization we carry out is a heterogeneous polymerization which generates a negligible amount of soluble PBMA polymer. The PBMA polymers precipitate from the continuous phase to form latex particles stabilized by PEO chains at their surface. To proceed more deeply into the analysis of the system at this point, a sample of the dispersion after 4 h of polymerization was freeze dried and redissolved in deuterated chloroform. PBMA is soluble in $CDCl_3$, and a clear solution is obtained. Figure 4 shows the ^{1}H NMR spectrum of this solution. We observe a reasonable spectrum for PBMA and for the other components of the system. We would like to stress two important points: First, the ^{1}H NMR spectrum in chloroform does not show any olefinic peaks due to the double bond of the macromonomer, even at amplified sensitivity, implying complete polymerization after 4 h of reaction. Second, the composition ratio of PBMA to PEO macromonomer calculated from the peaks in Figure 4 is completely consistent with their mole ratio in the feed. These two points, therefore, indicate that the disappearance of the macromonomer double bond peaks in the dispersions is not due to the adsorption of macromonomer to the latex surface. A gel permeation chromatogram (GPC) of this polymer solution also shows complete disappearance of macromonomer.

Table 2. Dispersion Copolymerization Results

polym time (min)	d_{eff}[a] (nm)	θ_M[b] (%)	θ_D[b] (%)	$[PEO]_{obs}$[c] (%)	$\Delta\nu_{1/2}(t)$[d] (ppm)	D[e] (nm)
0	0	0	0	100	0.021	
20	116	14	17	84	0.029	1.59
36	134	19	22	84	0.026	1.51
60	193	56	45	79	0.032	1.50
90	205	85	69	76	0.088	1.46
120	218	92	84	78	0.106	1.34
240	222	100	100	72		1.27

[a] Particle diameter as determined by dynamic light scattering. [b] Monomer (θ_M) and macromonomer (θ_D) conversion. [c] Observed fraction of the initial NMR signal intensity of the EO protons. [d] ^{1}H NMR line width of the olefinic protons of unreacted BMA. [e] Mean spacing between PEO anchor points, assuming all PEO chains are at the particle surface.

Another interesting point to be noted in Figure 3 is the presence of aliphatic protons in the region 0.5−2.5 ppm. These are not due to residual BMA monomer, and the signal is much too strong to be due to the hydrocarbon portions of the PEO macromonomer. The signal is consistent with a small amount of mobile PBMA groups. These may arise from a small amount of oligomer produced during the reaction, or alternatively, this signal may arise from BMA−macromonomer copolymer at the particle surface which is swollen by the solvent.[13] The signal detected corresponds to 4.0 ± 1.0 mol % of the PBMA segments.

Time−Conversion and Reactivity Ratio. From the areas of the vinylic protons, relative to those of the PCA standard, we can follow the extent of conversion of BMA (θ_M) and of the macromonomer (θ_D). These are calculated by the equation

$$\theta_i(\%) = \left[1.0 - \frac{(b_i/a)_t}{(b_i/a)_{t=0}}\right] \times 100 \qquad (1)$$

where $(b_i/a)_t$ is the ratio of the peak area of the double-bond protons of species i to that of the PCA protons at a given time (t) and $(b_i/a)_{t=0}$ is the corresponding value at $t = 0$. The experimental results are collected in Table 2, and time−conversion curves are shown in Figure 5. These sigmoidal curves are typical of those expected for a dispersion polymerization.[2] At early times, the polymerization rate of BMA is nearly the same as that of the macromonomer. Above 50% BMA conversion, however, BMA polymerization occurs faster than that of the macromonomer. This may be related to the locus of the monomer polymerization in the system.

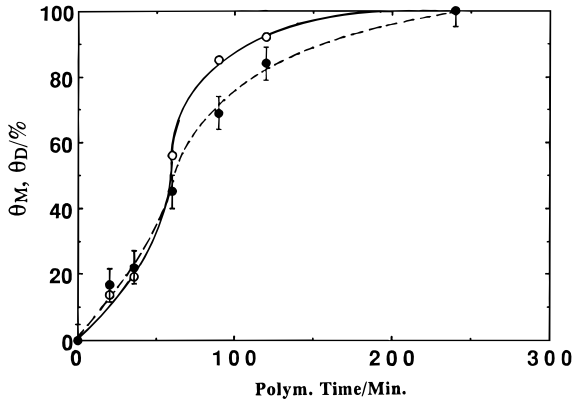

Figure 5. Time−conversion curves: (○) BMA; (●) C_1-EO_{53}-C_7-S. The bars represent the experimental error.

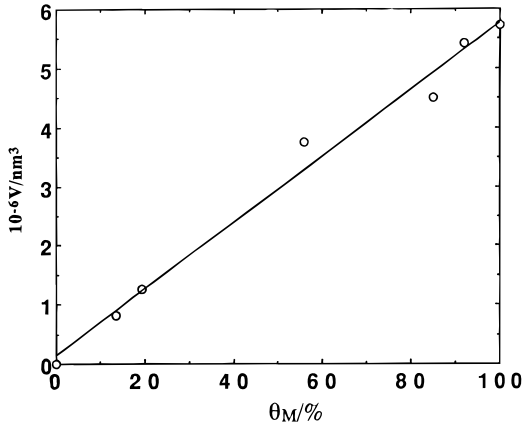

Figure 6. Plot of the mean particle volume, calculated from the DLS diameter, against the conversion of BMA (θ_M).

The copolymerization reactivity ratio (r_1) is given by

$$r_1 = \theta_M/\theta_D \tag{2}$$

where M_1 is BMA and M_2 is the macromonomer. When one uses the conversion values at 20 min of polymerization time, a value of $r_1 = 0.82 \pm 0.18$ is obtained. This value seems to be slightly high, when compared to the reference value of $r_1 = 0.55 \pm 0.10$,[14] where BMA is M_1 and styrene is M_2. That is, the apparent reactivity of the macromonomer, which is defined by $1/r_1$, decreases compared to that of styrene itself. This may be due to steric effects or to thermodynamic incompatibility between the macromonomer and the PBMA chain.[15−17] To obtain a more accurate value for r_1, we would have to determine its value at lower conversion, and before particle formation begins. Particle nucleation may have an important effect on the polymerizability of both BMA and the macromonomer.

In Figure 6 we examine particle size as a function of BMA conversion. We observe a linear relationship between BMA conversion (θ_M) and particle volume (V) determined by DLS, which implies that no secondary nucleation of particles occurs.[6]

Locus of Polymerization. NMR line widths are inversely proportional to the spin−spin relaxation time, T_2. The full line width at half-maximum ($\Delta\nu_{1/2}$) for a homogeneous solution is given by the equation[18]

$$\Delta\nu_{1/2} = \frac{1}{\pi}\left[\frac{1}{T_2} + \frac{1}{\Delta}\right] \tag{3}$$

where Δ contains the contributions to the magnetic field inhomogeneity resulting from the equipment used and sample properties (concentration and viscosity). The values are listed in Table 2. To compare BMA with PCA, the values are normalized by the equation

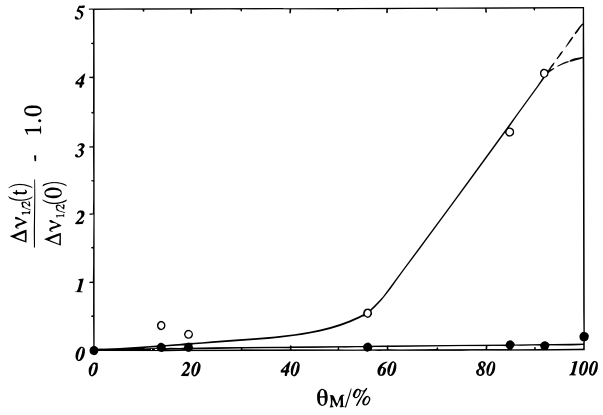

Figure 7. Plots of NMR half-height line width of vinyl protons of BMA (○) and PCA protons (●) at polymerization time (t), normalized to that at $t = 0$, vs the conversion of BMA (θ_M).

$$Q = \frac{\Delta\nu_{1/2}(t)}{\Delta\nu_{1/2}(0)} - 1.0 \tag{4}$$

In Figure 7, we plot values of Q for the double-bond peaks of BMA, and for the PCA protons, against the conversion of BMA. As the viscosity of the continuous medium increases, which corresponds to the increase in latex diameter, there is a small broadening of the PCA proton line widths. In contrast to the PCA, the line widths of the BMA vinyl protons increase significantly, particularly at 50% conversion. When there is rapid exchange of BMA molecules in different physical environments, the relaxation rates of the different states are dynamically averaged, and therefore additive.[10] In the present dispersion, free BMA molecules (c) in the continuous phase and adsorbed BMA (a) in the latex interior have widely different rates, indicated by T_{2c} and T_{2a}, respectively. The average BMA relaxation time T_2 is then given by

$$\frac{1}{T_2} = \frac{(1 - f_a)}{T_{2c}} + \frac{f_a}{T_{2a}} \tag{5}$$

where f_a is the fraction of time the BMA molecule spends in the latex interior. The increase in line width indicates that a significant amount of the BMA has partitioned into a higher viscosity environment, which can be identified as the particle interior, and that the strong increase in Q implies the increase in f_a. That is, above 50% conversion residual BMA molecules prefer to be in the latex interior, rather than in the continuous phase. Because of both enhanced local concentration and the onset of the gel effect, the polymerization rate of BMA in the particles is much faster than in the bulk. The steep increase in the BMA conversion rate seen in Figure 5 corresponds to the prominence of polymerization within the particles, with additional monomer supplied by BMA in the bulk. In other words, there is a change in the locus of polymerization in the reaction.

Fate of the Macromonomer. The intensity of the PEO protons was followed as a function of polymerization time. A very interesting observation is that at partial conversion, there is a net decrease in intensity of the sharp PEO signal, accompanied by signal broad-

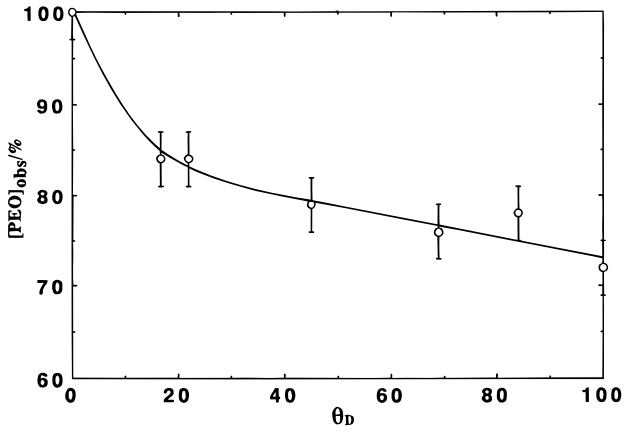

Figure 8. Plot of $[PEO]_{obs}$, the relative intensity of the ^1H NMR signal of the PEO protons, vs conversion of C_1-EO_{53}-C_7-S macromonomer (θ_D). The error bars represent one standard deviation.

ening at the base of the peak. This broad component is difficult to discern in the spectrum for reaction times shorter than 2 h, but by the end of the reaction, its presence is clearly apparent. As shown in the insert in Figure 3, this broad band has a width at half-height of ca. 160 Hz.

Rigorous quantitative analysis of this band is difficult, because it appears in the same region of the spectrum as the weak signals due to PBMA. The center of the band is downfield from the main PEO peak, implying a somewhat different chemical shift. It does appear at this point in the conversion that all of the ^1H signal from the EO segments can be detected. In this spectrum, approximately 75% of the EO signal intensity appears in the sharp peak. We take this result to indicate that there is a clear separation in signal of the partially immobilized PEO from the very mobile segments that appear in the sharp peak at 3.64 ppm.

To quantify the changes which occur in the PEO signal, we follow the decrease in the intensity of the sharp peak at 3.64 ppm, which can be determined with good precision, relative to that of the PCA reference. This intensity change, expressed in terms of the percent of the initial PEO peak intensity ($[PEO]_{obs}$), can be calculated through the expression

$$[PEO]_{obs}\ (\%) = \frac{[(PEO)/a]_t}{[(PEO)/a]_{t=0}} \times 100 \qquad (6)$$

where $[(PEO)/a]_t$ and $[(PEO)/a]_{t=0}$ are the peak area ratios of the 3.64 ppm signal to those of the PCA protons, at polymerization times t and $t = 0$, respectively.

In Figure 8, values of $[PEO]_{obs}$ are plotted against the conversion of macromonomer. Over the first 20% of reaction, the intensity in the sharp PEO peak decreases to about 85% of the intensity initially present in the system. With subsequent reaction, this amount decreases more slowly, and by the end of the reaction, about 73 ± 3% of the PEO protons can be detected in the NMR spectrum in the sharp peak at 3.64 ppm. Our interpretation of this result is that at the end of the reaction, 25−30% of the PEO protons have become immobilized and now appear within the broad band seen in the insert in Figure 3.

PEO Chains at the Particle Surface. It is possible to take the data in Figure 8 and to draw from them some insights into the conformation of the PEO chains covalently attached at the particle surface. This requires some additional assumptions. A useful assumption in our model is that after the particle number has become constant, there is little adsorption of free macromonomer onto the particle surface.

We know from independent experiments in water that PEO chains adsorb weakly to the surface of PBMA particles stabilized by a low surface concentration of sulfate groups. PBMA macromonomer adsorbs more strongly, exhibiting a classic Langmuir isotherm, with an area per chain at saturation of 2.0 nm^2. It is likely that at these densities, adsorption is dominated by interaction of the hydrophobic tail of the macromonomer with the hydrophobic surface of the PBMA latex. The mean separation between polymers at this surface coverage (1.6 nm) is smaller than the spacing estimated from the radius of gyration of the PEO chain ($2R_G$ = 3.2 nm in methanol for this chain length,[19] with a similar value for water). This adsorption density will lead to some stretching of the PEO chains.[10] In aqueous methanol, we expect the hydrophobic interaction between the chain end and the particle surface to be somewhat weaker than that in water.

A second assumption we need to make is that polymerized macromonomer is incorporated into the particles and not present as soluble oligomer. We have some GPC and NMR evidence to support this assumption at the end of the reaction. With these two assumptions, we calculate at 20 min reaction time, where the number of particles in the reaction has become constant, that the small value of $[PEO]_{obs}$ corresponds to immobilization of 83 ± 11% of the polymerized PEO. Since we monitor both particle size and monomer conversion, we can calculate that the mean spacing (D) between PEO chains incorporated into the particles, at θ_D = 17%, is 1.6 nm. The high degree of immobilization, and the relatively large spacing between chains, suggest that the PEO chains tend to lie flat on the particle surface. Some macromonomer adsorption here could also contribute to immobilization of PEO chains. At the end of the reaction, the mean particle spacing is much smaller and corresponds to D = 1.27 nm if all PEG chains remain at the particle surface.

To examine the immobilization process more quantitatively, we define the mobile fraction f_M of PEO chains incorporated into the particles at each extent of macromonomer conversion. We calculate f_M as the ratio of NMR-detectable protons of anchored PEO chains at 3.64 ppm, to the total extent of PEO macromonomer conversion

$$f_M = \frac{[PEO]_{obs} - (100 - \theta_D)}{\theta_D} \qquad (7)$$

This value increases with increasing extent of monomer and macromonomer conversion, indicating that an increasing fraction of the PEO chains incorporated into the particles become mobile enough to contribute to the 3.64 ppm peak in the NMR spectrum. In Figure 9 we plot values of f_M vs the calculated interchain spacing D.

There are two different types of explanations for the changes in f_M. First, at low conversion, the surface coverage of the particles may be sparse enough that the PEO chains can loop back to adsorb onto the surface, rendering portions of the chains relatively immobile.[20] Alternatively, each chain may be anchored at a different depth in the surface, with only the portions of the chain

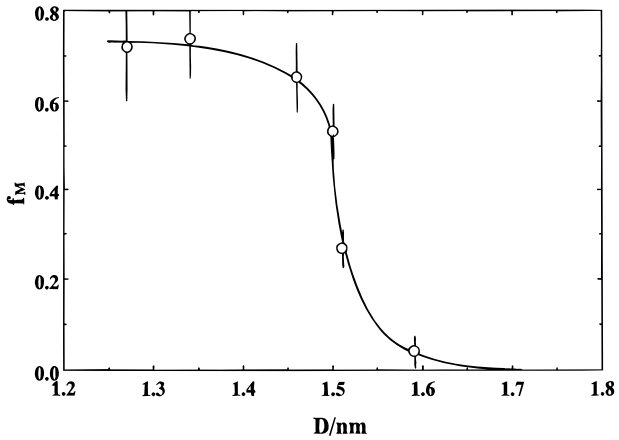

Figure 9. Plot of mobile fraction (f_M) of surface-anchored PEO chains against the estimated mean separation D between PEO anchor points on the surface of the particles. The D values are calculated from the particle size and number, assuming that all PEO chains are located at the surface.[6] The error bars represent the one standard deviation in the experimental error. Note that large D values refer to low conversion and high D values, to high conversion.

extending from the surface mobile enough to be detected by NMR. In the context of both explanations, as monomer conversion proceeds, there is a decrease in the mean separation between chains at the particle surface.

In Figure 9, values of f_M increase sharply with decreasing D in the range of about 70% macromonomer conversion. Here and at higher conversions, the values of D are smaller than the mean separation ($2R_G = 3.2$ nm in methanol[19]) anticipated for random PEO coils at the particle surface. This is the range of anchor point separations where one anticipates chain stretching. The sharpness of the transition in the f_M vs D plot is very interesting in that respect, because it suggests that we are observing the onset of a pancake-to-brush transition. For example, in dynamic light scattering studies of adsorption of PEO to colloidal particles, one observes a sharp increase in hydrodynamic radius as the surface becomes saturated with polymer,[21,22] consistent with a transition to a brushlike surface structure for the adsorbed chains.

The D values in Figure 9 are calculated by assuming that all reacted macromonomer is located at the particle surface throughout the polymerization reaction. If some of the immobilized PEO segments are due to entire polymer molecules buried in the particle interior, then the actual values of D on the x-axis in Figure 9 will be somewhat larger, but the general features of our conclusions will not change.

Nature of the Immobilized PEO Segments. At the end of the polymerization reaction, some 25−30% of the PEO signal appears as a very broad peak, as seen in Figure 3. This signal is due to immobilized segments of the polymer. There are two ways in which one can imagine these segments to be immobilized. First, a fraction of the PEO chains could be trapped inside the particle during the polymerization reaction. This is the situation depicted in Figure 1C. Here the broad signal would contain contributions from entire polymer chains buried inside the particle. This was, initially, our hypothesis about the reaction. Alternatively, the PEO chains might all be near the surface but anchored at different depths, perhaps as depicted in Figure 1B.

In this type of particle, one might anticipate a diffuse interface between the corona chains, which extends into the continuous medium, and the solid polymer particle phase. The mobile PBMA segments in the particle support this picture. If this were the case, the least mobile segments would be those anchored deepest into the PBMA phase. The segments which protrude through the diffuse interface become more mobile. Even those segments in the corona but close to the interface would have a restricted mobility, as pointed out many years ago by Douglass and McBrierty.[23] This situation would lead to a distribution of mobilities for the immobilized PEO chains and still leave the vast majority of the segments in a highly mobile environment. In this context, the much larger fraction of immobilized *particle-bound* segments observed at early conversions can be explained as suggested above in terms of surface adsorption leading to loops and trains when the D values are small. This point of view is not rigorously established, but it is consistent with the data.

Conclusions

We report a ^{1}H NMR study of dispersion copolymerization of BMA with PEO macromonomer in deuterated aqueous methanol. The time−conversion of both BMA and macromonomer were followed, allowing the reactivity ratio ($r_1 = 0.82 \pm 0.18$, where M_1 is BMA and M_2 is the macromonomer) to be determined. The NMR line width of the unreacted BMA increases sharply above 50% of conversion of BMA, as does the BMA polymerization rate, implying transfer of the BMA molecules from the continuous medium to the latex particle interior. As the reaction proceeds, some of the intensity of the PEO signal disappears from the sharp peak at 3.64 ppm and is accompanied by a new broad peak at its base. This new signal is assigned to PEO segments which become immobilized in the solid polymer particle phase. The intensity of the sharp PEG signal due to particle-bound PEG indicates a sudden increase in PEO chain mobility at high macromonomer conversion. This corresponds to a point in the reaction where the mean spacing between chains at the particle surface becomes significantly smaller than $2R_G$, a classic signature of a transition to a brushlike conformation for the PEO chains at the particle surface.

Acknowledgment. The authors would like to thank ICI, ICI Canada, The Glidden Co., and NSERC Canada for their support of this research. The authors also thank Mrs. E. Odrobina at the University of Toronto for the binding isotherm measurements. S.K. would like to express his grateful acknowledgment to the Ministry of Education, Science, and Culture of Japan for supporting his stay in Toronto.

References and Notes

(1) Permanent address: Department of Materials Science, Toyohashi University of Technology, Tempaku-cho, Toyohashi, 441 Japan.
(2) Candau, F., Ottewill, R., Eds. *An Introduction to Polymer Colloids*; Kluwer Academic Press: Dordrecht, Netherlands, 1990.
(3) Barret, K. E. J. *Dispersion Polymerization in Organic Media*; Wiley-Interscience: New York, 1975.
(4) Egan, L. S.; Winnik, M. A.; Croucher, M. D. *Langmuir* **1988**, *4*, 438.
(5) Winnik, F. M.; Paine, A. J. *Langmuir* **1989**, *5*, 903.
(6) Kawaguchi, S.; Winnik, M. A.; Ito, K. *Macromolecules* **1995**, *28*, 1159.
(7) Paine, A. J. *Macromolecules* **1990**, *23*, 3109.
(8) Cosgrove, T.; Griffiths, P. C. *Adv. Colloid Interface Sci.* **1992**, *42*, 175.
(9) Blum, F. *Colloids Surf.* **1990**, *45*, 361.

(10) Fleer, G. J.; Cohen Stuart, M. A.; Scheutjens, J. M. H. M.; Cosgrove, T.; Vincent, B. *Polymer at Interfaces*; Chapman & Hall: London, 1993.
(11) Barnett, K. G.; Cosgrove, T.; Vincent, B.; Sissons, D. S.; Cohen-Stuart, M. *Macromolecules* **1981**, *14*, 1018.
(12) (a) Alexander, S. *J. Phys. (Paris)* **1977**, *38*, 983. (b) de Gennes, P. G. *Macromolecules* **1980**, *13*, 1069.
(13) (a) van der Put, A. G.; Bijsterbosch, B. H. *J. Colloid Interface Sci.* **1983**, *92*, 499. (b) Goossens, J. W. S.; Zembrod, A. *Colloid Polym. Sci.* **1979**, *257*, 437.
(14) Brandrup, J.; Immergut, E. H. *Polymer Handbook*, 3rd ed.; Wiley: New York, 1989.
(15) (a) Ito, K.; Tsuchida, H.; Kitano, T.; Yamada, E.; Matsumoto, T. *Polym. J.* **1985**, *17*, 827. (b) Ito, K.; Tsuchida, T.; Kitano, T. *Polym. Bull.* **1986**, *15*, 425. (c) Ito, K.; Yokoyama, S.; Arakawa, F.; Yukawa, Y.; Iwashita, N.; Yamasaki, Y. *Polym. Bull.* **1986**, *16*, 337.
(16) Tsukahara, Y.; Tanaka, M.; Yamashita, Y. *Polym. J.* **1987**, *19*, 1121.
(17) Kennedy, J. P.; Hiza, H. *J. Polym. Sci., Polym. Chem. Ed.* **1983**, *21*, 1033.
(18) Abraham, R. J.; Loftus, P. *Proton and Carbon-13 NMR Spectroscopy*; Heyden & Son Ltd.: Chichester, U.K., 1978.
(19) Zhou, P.; Brown, W. *Macromolecules* **1990**, *23*, 1131.
(20) Cohen-Stuart, M.; Cosgrove, T.; Vincent, B. *Adv. Colloid Interface Sci.* **1986**, *24*, 143.
(21) Killmann, E.; Sapuntzjis, P. *Colloids Surf. A: Physicochem. Eng. Aspects* **1994**, *86*, 229.
(22) Killmann, E. *Macromol. Chem., Macromol. Symp.* **1988**, *17*, 57.
(23) Douglass, D. C.; McBrierty, V. J. *Polym. Eng. Sci.* **1979**, *19*, 1054.

MA950726T